Supplementary Information (SI) for Physical Chemistry Chemical Physics.
This journal is © the Owner Societies 2026

First-Principles Investigation of the Insulator–Metal Transition in Layered $NaNiO_2$: Coupled Electronic and Lattice Effects

Xiaohong Chu, Zhenyi Jiang*, Ping Guo*, JimingZheng, Xiaodong Zhang
Shaanxi Key Laboratory for Theoretical Physics Frontiers, Institute of Modern Physics, Northwest University, Xi'an 710069

Description of Crystal Cell Re-built

To ensure consistency throughout all calculations, the original unit cell was redefined. This was achieved by taking integer combinations of the original lattice vectors, yielding a new set of lattice vectors while preserving both the lattice framework and the atomic topology. Let the original lattice vector matrix be L (with column vectors), and the new lattice vector matrix be L'. They are related through an integer transformation matrix P as $L' = LP$. Assuming the original lattice vectors (in Å) are given by:

$$L = \begin{bmatrix} 1 & 0 & 0 \\ 0 & 1 & 0 \\ 1 & 0 & 1 \end{bmatrix}$$

For $C2/m$:

$a_1=1/2(a+b)$
$b_1=1/2(-a+b)$
$c_1=3c$

For $R\bar{3}m$:

$a_1=a$
$b_1=b$
$c_1=b+c-a$

Through the above operations, a new crystal cell matrix is obtained.

Van Vleck model analysis of Jahn–Teller distortions in NiO_6 octahedra

To quantitatively analyze the Jahn–Teller distortion of the NiO_6 octahedron, we employed the Van Vleck model, in which the six Ni–O bond lengths of the octahedron are expanded into symmetry-adapted modes. The specific procedure is as follows:

The six Ni–O bonds are averaged along the local x, y, and z directions to obtain l_x, l_y, and l_z, respectively. Among these, the E_g modes of the octahedron correspond to two distinct displacement patterns. Axial tetragonal mode (Q_3): elongation or compression along the z-axis, which breaks axial symmetry;
Transverse orthorhombic mode (Q_2): unequal bond lengths within the xy-plane, which breaks planar symmetry.
The corresponding expressions are given as:

$$Q_2 = \frac{1}{\sqrt{2}}(l_x - l_y) \quad , Q_3 = \frac{1}{\sqrt{6}}(2l_z - l_x - l_y)$$

Here, the calculated values are $Q_2 = 0$ and $Q_3 = 0.2397$Å.

The coefficients and their summation are determined by the normalization conditions in group theory, ensuring that the two modes are orthogonal and independent in the energy expansion.
When $Q_3 > 0$ and $Q_2 \approx 0$, the system corresponds to a typical axial Jahn–Teller distortion, characterized by

two elongated bonds and four shortened bonds;
When $Q_2 \neq 0$, unequal bond lengths emerge within the *xy*-plane, indicating the presence of an orthorhombic Jahn–Teller component.

The description regarding the calculation of the g-factor

Based on perturbation theory for the *g* factors of a d^7 configuration in a tetragonally distorted octahedron, the calculated results show a pronounced variation in the *g*-factor anisotropy during the phase transition, providing supporting evidence for the characteristics of the IMT. The *g*-factor is calculated using the following formula[1,2]:

$$g_{//} = g_s \square 2k'\zeta' / E_{1//}^2$$
$$g_{\square} = g_s \square 2k'\zeta' / E_{1\square}^2 \square 3k\zeta / E_{\square}$$

Among them,

$$E_{\square} = / E_{3\square} \square 1 / E_{4\square} \square 0.38(1 / E_{3\square} \square 1 / E_{4\square})$$

Here, E_i represents the energy difference between the ground and excited states, while the subscripts // and ⊥ correspond to the axial and perpendicular components of the tetragonal splitting of the relevant energy levels. These values can be obtained from the energy matrix of a d^7 ion under tetragonal symmetry:

$$E_{1//} = 10D_q \square 4B \square 4C$$
$$E_{1\square} = 10D_q \square 4B \square 4C \square 3D_s \square 5D_t$$
$$E_{3\square} = 10D_q \square 6B \square C \square 3D_s \square 5D_t$$
$$E_{4\square} = 10D_q \square 14B \square C \square 3D_s \square 5D_t$$

In the above formula, the spin-orbit coupling coefficients (ζ and ζ') and the orbital reduction factors (k and k') arise from the anisotropic (diagonal and off-diagonal) interactions of the spin-orbit coupling and orbital angular momentum operators within the irreducible representation γ. Within the cluster approach, these quantities are expected to satisfy the following relationships[3,4]:

$$\zeta = N_t(\zeta_d^{\,0} + \lambda_t^{\,2}\zeta_p^{\,0} / 2), \qquad \zeta' = (N_t N_e)^{1/2}(\zeta_d^{\,0} - \lambda_t\lambda_e\zeta_p^{\,0} / 2),$$
$$k = N_t(1 + \lambda_t^{\,2} / 2), \qquad k' = (N_t N_e)^{1/2}[1 - \lambda_t(\lambda_e + \lambda_s A) / 2].$$

ζ_d^0 and ζ_p^0 represent the orbital coupling coefficients of $3d^7$(Ni^{3+}) and ligand (O^{2-}), respectively. A is the integral $R\langle ns|\partial/\partial y|npy\rangle$, based on the reference distance R. N_γ , λ_γ and λ_s are normalization factors and orbital mixing coefficients. The normalization factor satisfies:

$$N_t\left(1 - 2\lambda_t S_{dpt} + \lambda_t^2\right) = 1,$$
$$N_e\left(1 - 2\lambda_e S_{dpe} - 2\lambda_s S_{ds} + \lambda_e^2 + \lambda_s^2\right) = 1,$$
$$N^2 = N_t\left(1 + \lambda_t^2 S_{dpt}^2 - 2\lambda_t S_{dpt}\right),$$
$$N^2 = N_e\left(1 + \lambda_e^2 S_{dpe}^2 + \lambda_s^2 S_{ds}^2 - 2\lambda_e S_{dpe} - 2\lambda_s S_{ds}\right).$$

In the formula, N represents the degree of covalency (covalent factor) between the central Ni^{3+} and the ligand O^{2-}. S_{dp} and S_{ds} are group overlap integrals, which are proportional to the orbital mixing coefficients: $\lambda_e/S_{dpe} \approx \lambda_s/S_s$.

References

1. Y. Tanabe, S. Sugano, *J. Phys. Soc. Japan*, 1954, 9, 766-779.
2. D. J. Newman, B. Ng, Rep. Prog. Phys. 1989, 52, 699.
3. A. Agarwal, A. Sheoran, S. Sanghi, *Spectrochim Acta A*. 2010, 75, 964-969.
4. C. C. Ding, L. Jia, X. Wang, *Phys. Chem. Solids*. 2021, 150, 109800.

Table S-1. Crystal structures and energies obtained from soft-mode structural exploration of the high-temperature $R\bar{3}m$ phase.

q-points	Irreducible Representation	Frequency (THz)	Relaxed Space Group	*E* (eV/f.u.)
Γ	Γ_3^+	-1.643	$P2_1/c$	-19.263
M	M_3^+	-4.863	$P2/m$	-19.135
M	M_5^-	-4.852	$R\text{-}3m$	-19.293
A	A_1^-	-2.008	$C2/c$	-19.237
L	L_2^-	-4.789	$R\text{-}3m$	-19.293
L	L_2^- (the other component)	-4.776	$R\text{-}3m$	-19.293

Table S-2. Energetics of different magnetic states.

Magnetic Configuration	*E* (eV/f.u.)
A-AFM	-19.4485
C-AFM	-19.4487
G-AFM	-19.4519
FM	-19.4503

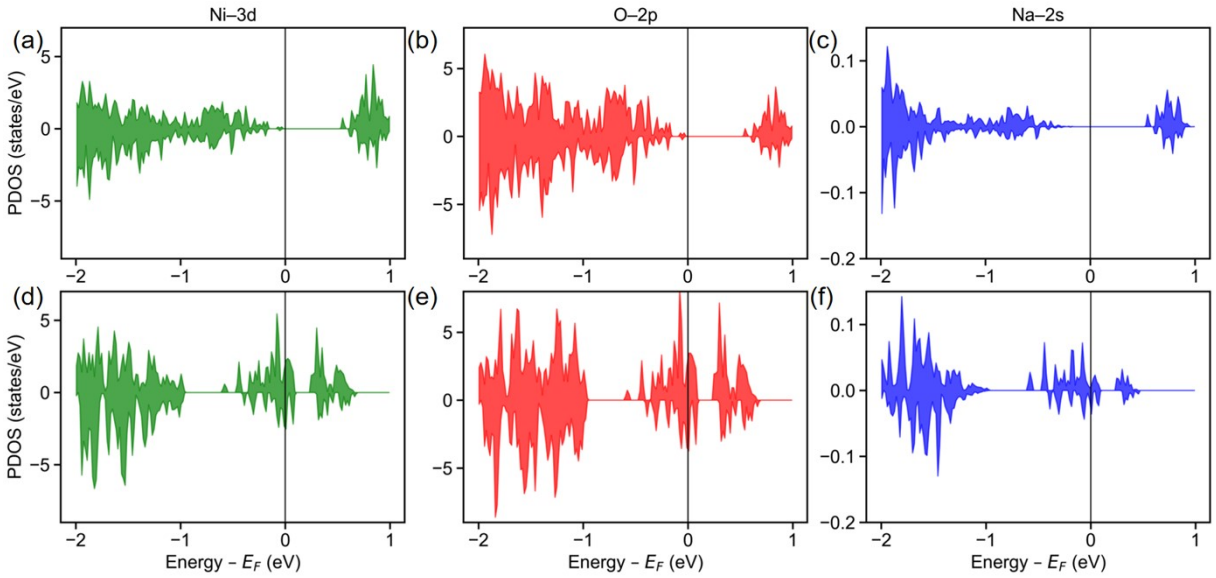

Fig. S-1. Projected density of states (PDOS) for the low-temperature monoclinic $C2/m$ phase: (a) Ni-3d, (b) O-2p, and (c) Na-2s orbitals; and for the high-temperature rhombohedral $R\bar{3}m$ phase: (d) Ni-3d, (e) O-2p, and (f) Na-2s orbitals.

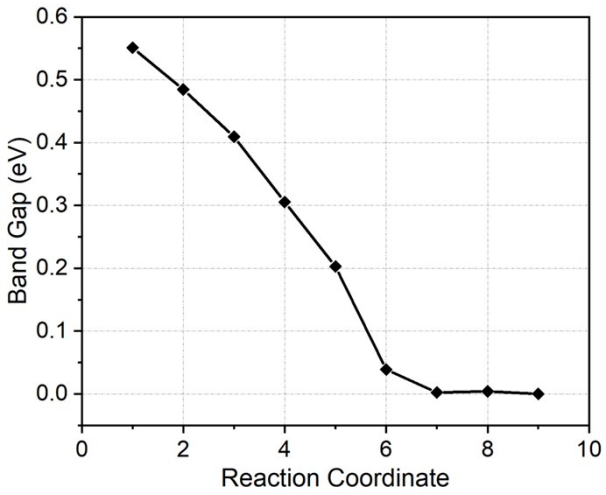

Fig. S-2. Variation of the band gap during the distortion process.

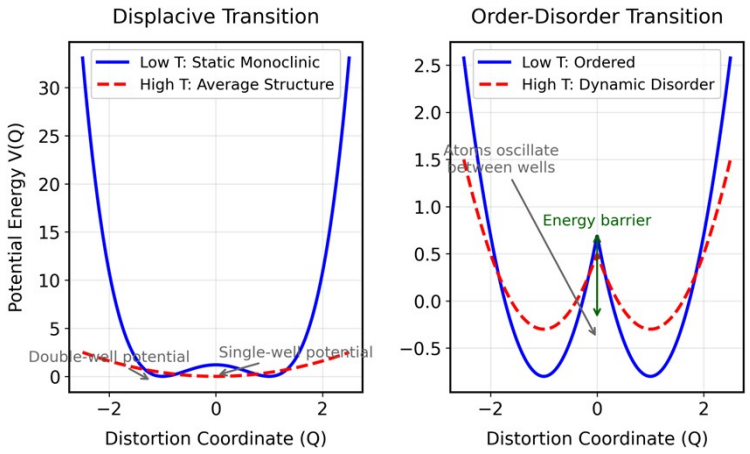

Fig. S-3. This illustrates simple examples of displacive and order–disorder transitions. In this work, it has no specific physical significance and is used solely to highlight the difference between the two types of phase transitions.

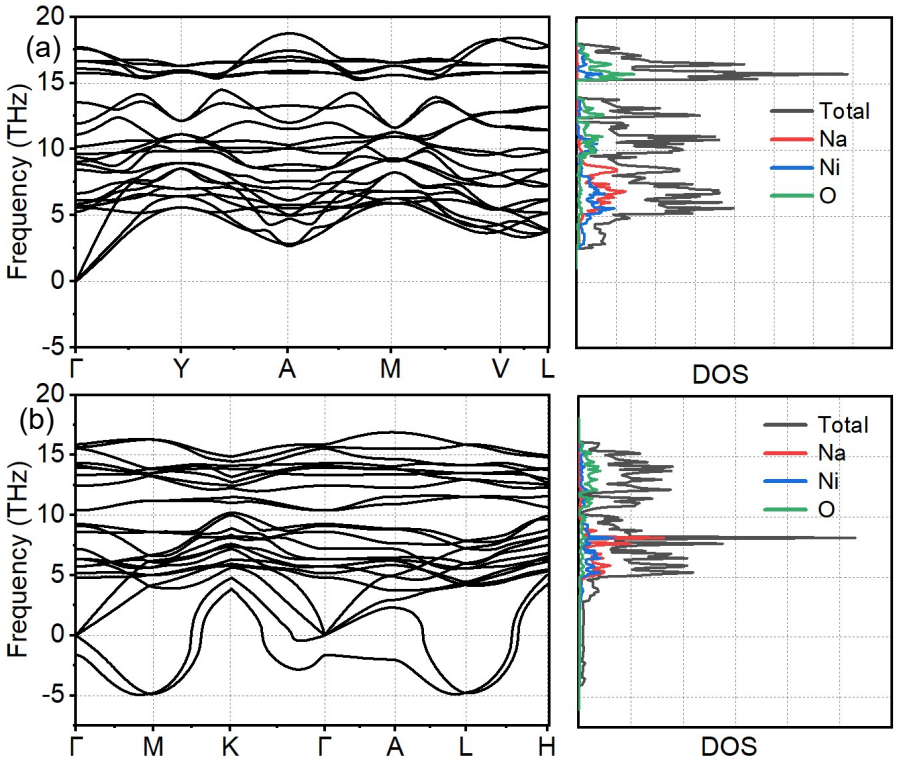

Fig. S-4. Phonon spectra of (a) the low–temperature monoclinic $C2/m$ phase and (b) the high–temperature rhombohedral $R\bar{3}m$ phase.

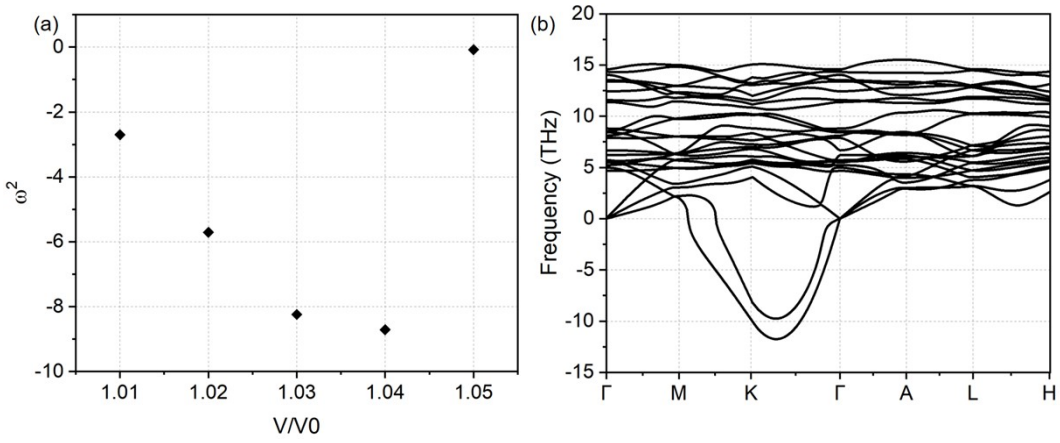

Fig. S-5. Regulation of phonon instability in the high-temperature rhombohedral phase by thermal expansion. (a) Pronounced suppression of the dynamical instability at the Γ point. The squared frequency (ω^2) of the softest optical phonon mode at Γ as a function of the relative volume (V/V_0). (b) Transfer of instability modes. Phonon spectrum corresponding to the largest volume in (a) ($V/V_0 = 1.05$). The imaginary frequency at the Γ point is strongly suppressed; however, dynamical instabilities persist at specific non-Γ wave vectors in the Brillouin zone, indicating that the instability of the high-temperature phase is not completely eliminated but instead shifts to spatially modulated modes.

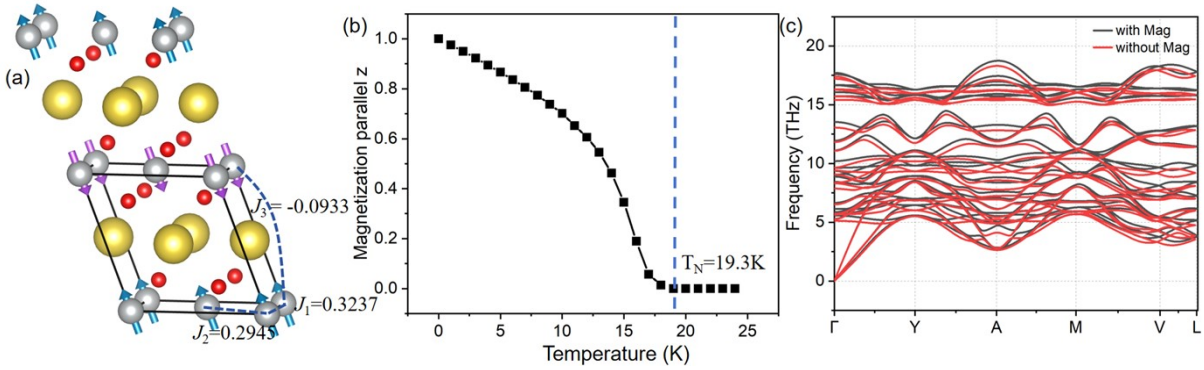

Fig. S-6. Low-temperature properties of $NaNiO_2$, including (a) the A-type antiferromagnetic magnetic configuration, Large yellow spheres denote Na, gray spheres Ni, and red spheres O.(b) the calculated Néel temperature (~19.3 K), and (c) a comparison of the phonon spectra obtained with and without magnetic ordering.

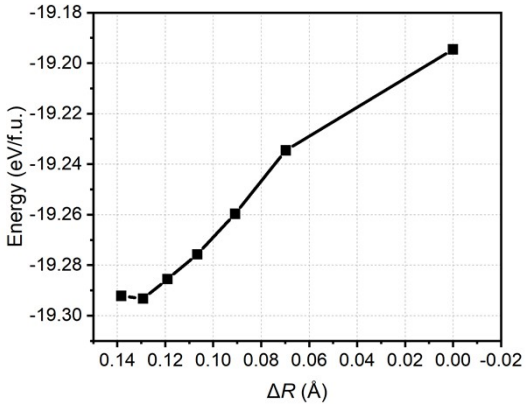

Fig. S-7. Evolution of the energy per formula unit (eV/f.u.) as a function of the bond-length difference index (ΔR). The

horizontal axis (ΔR) quantifies the degree of local structural distortion, defined as the difference between the longest and shortest Ni–O bond lengths in each NiO_6 octahedron.